Tsunami Resonance Characterization in Japan due to Transpacific sources: Response on the Bay and Continental Shelf

Y. Wang[1,2], N. Zamora[2,3], M. Quiroz[2,4], K. Satake[1] and R. Cienfuegos[2,4]

[1] Earthquake Research Institute, The University of Tokyo, Tokyo, Japan.

[2] Centro de Investigación para la Gestión Integrada del Riesgo de Desastres (CIGIDEN), ANID/FONDAP/1511007, Santiago, Chile.

[3] CYCLO - Millennium Nucleus the seismic cycle along subduction zones, Valdivia, Chile.

[4] Departamento de Ingeniería Hidráulica y Ambiental, Escuela de Ingeniería, Pontificia Universidad Católica de Chile, Santiago, Chile.

NH5.1 – Tsunamis EGU2020-4021

1. Aim of our Study

To assess the resonance processes from transoceanic and local sources in the ports of the Hokkaido and Sanriku regions in Japan.

- We analyze the characteristics of the resonance behavior based on past events..
- We use spectral analysis. The spectrum allows us to identify the total energy distributed in the periods and compare those relative peaks that are important.
- We also calculate the theoretical free oscillation modes of each region.

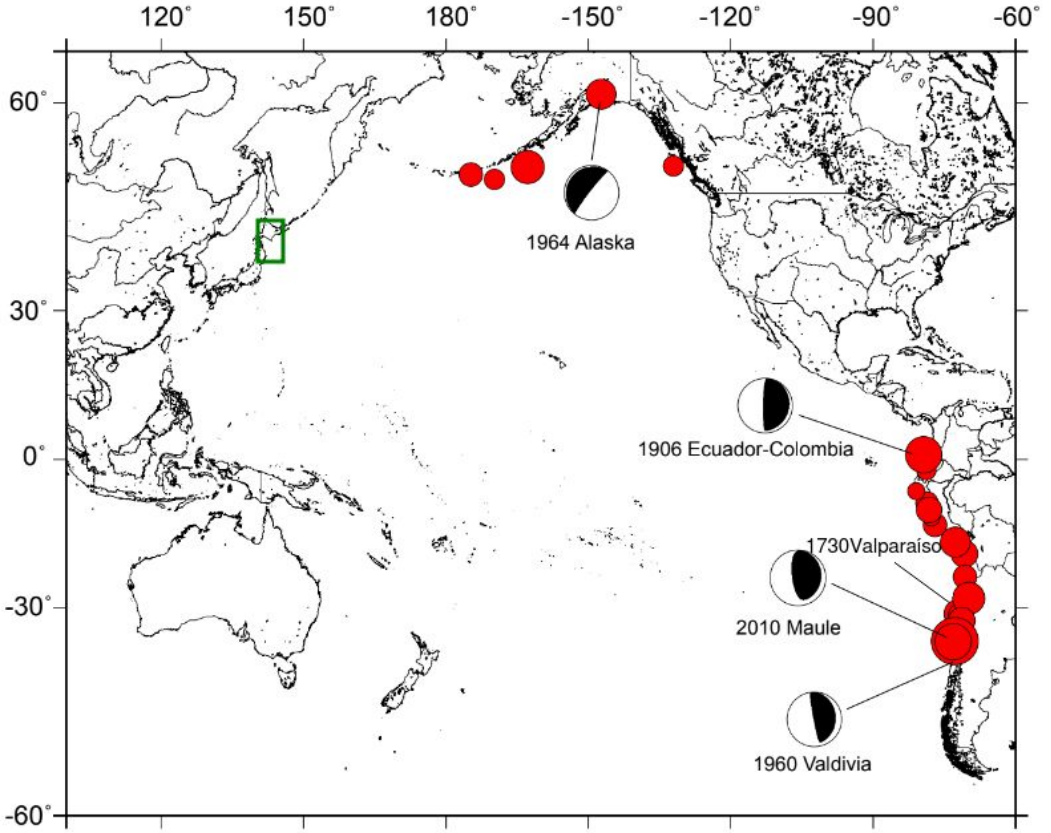

2. Data and Methods

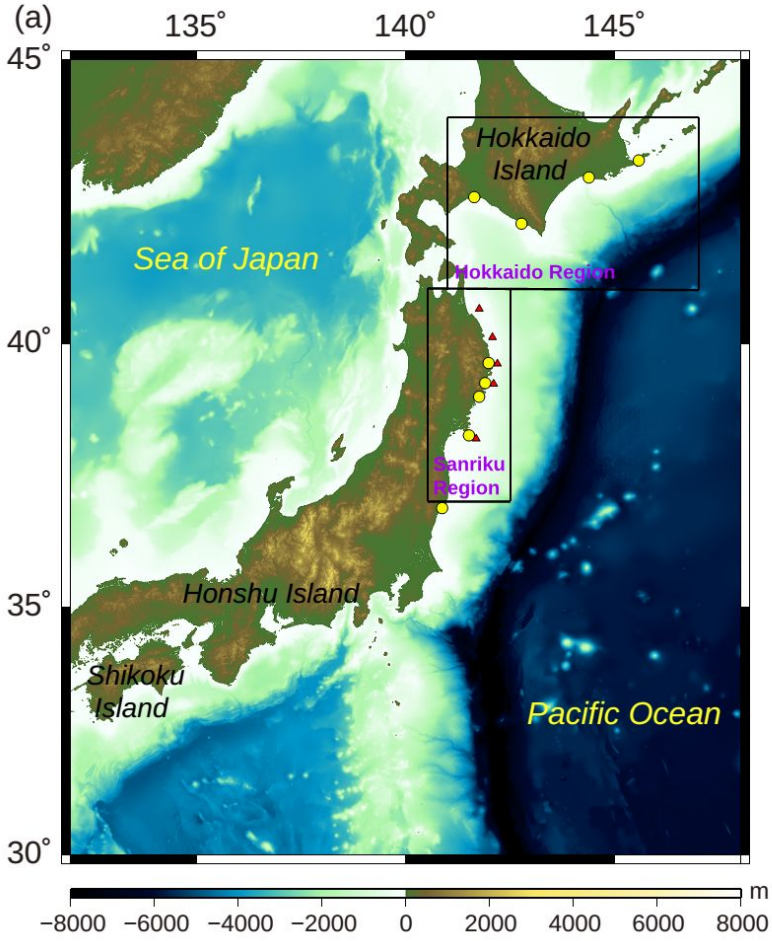

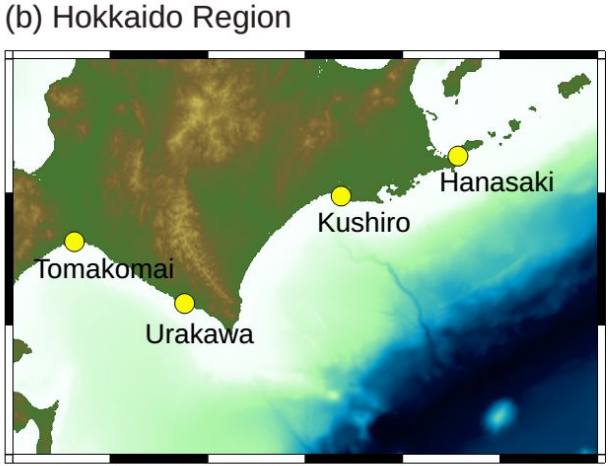

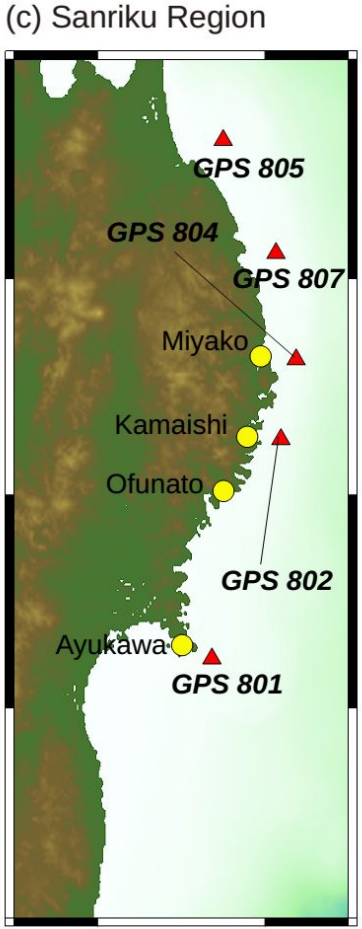

Hokkaido Region

Tide Gauge (4): Hanasaki, Kushiro, Urakawa, Tomakomai

Sanriku Region

Tide Gauge (4) : Miyako, Kamaishi, Ofunato, Ayukawa

GPS Gauge (5): 805, 807, 804, 802, 801

2. Data and Methods

Spectral Analysis:

Wavelet analysis is applied based on the package given by (Torrence and Compo, 1998), and its complex form, $\Psi(t)$, is:

$$\Psi(t) = A\frac{1}{\sqrt{\pi}}e^{-t^2}e^{2\pi it}$$

Where A is a normalization constant. The continuous wavelet transform of the signal as a function of scale and shift is given by Tang et al. (2008).

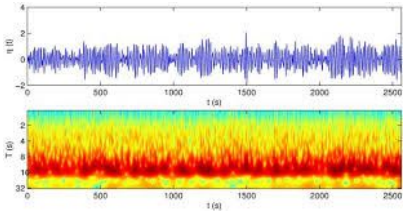

Modal Analysis:

The free modes of oscillations in tsunami amplification at the coast are calculated by modal analysis approach (Bellotti et al., 2012). It solves the eigenvalues associated to the homogeneous Linear Shallow Water Equations (LSWE) in a finite element grid, and numerically calculates the natural frequencies. A full reflection and an approximate radiation condition are assumed at the coastal and open boundaries.

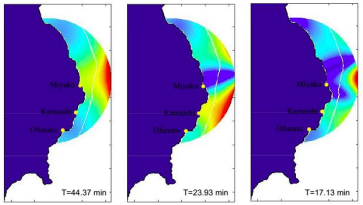

3. Results: Spectral Analysis of Tide Gauges at Hokkaido Region

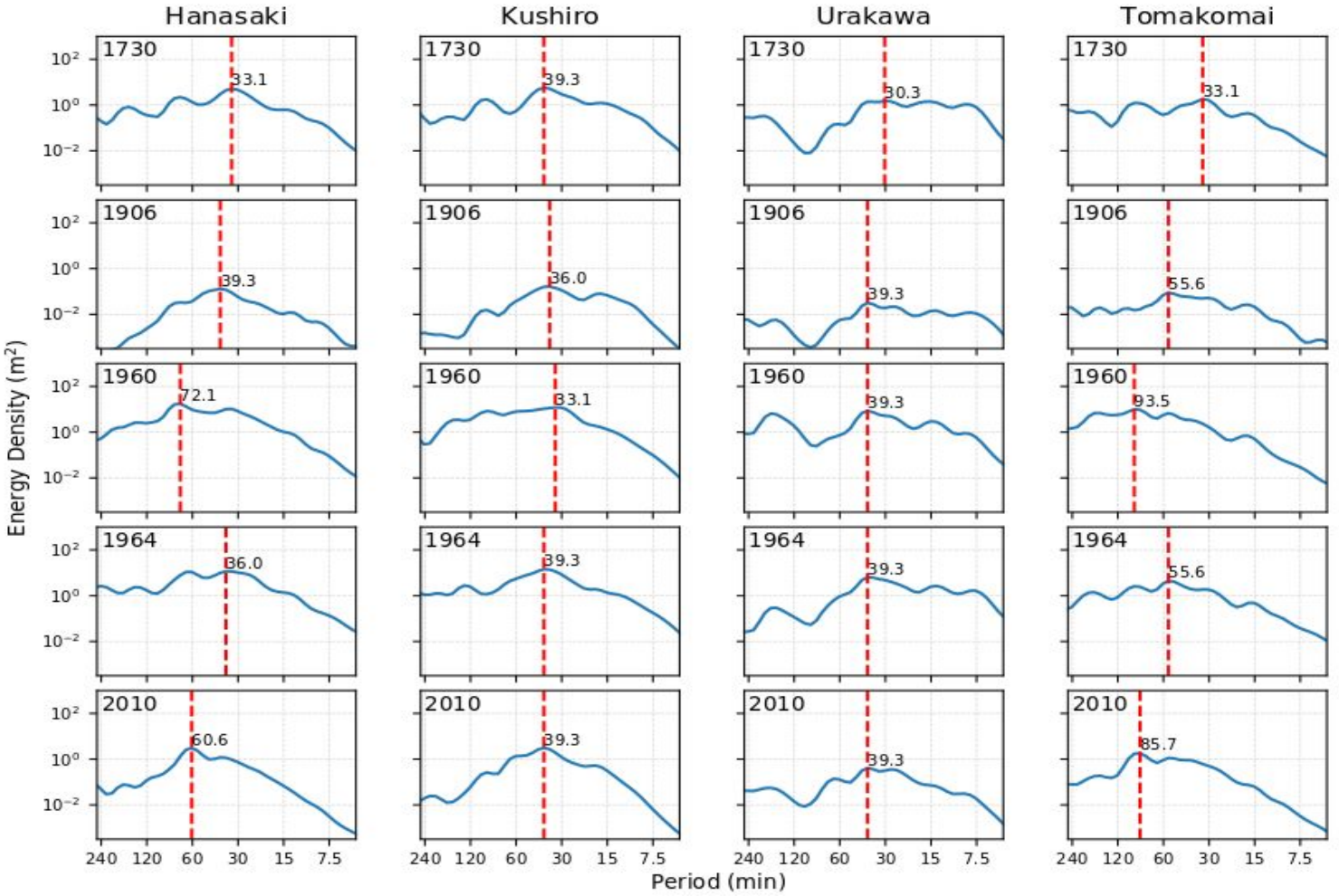

Hanasaki: **All tsunami events have similar frequency response** (33.1 min to 39.3 min).

Kushiro: **The 1960 tsunami event has a different response from other events** (50 min to 120 min). However, for the other four tsunami events, the dominant periods are 30 min to 80 min.

Urakawa: **Five tsunami events have different behaviors on the spectrum.** The energy of the 1960 event concentrates in the high–period (low-frequency) part, with a predominant period of 157.2 min. But for the 1964 and 2010 events, the peak of the spectrum is around 40 min.

Tide Gauges at Hokkaido Region

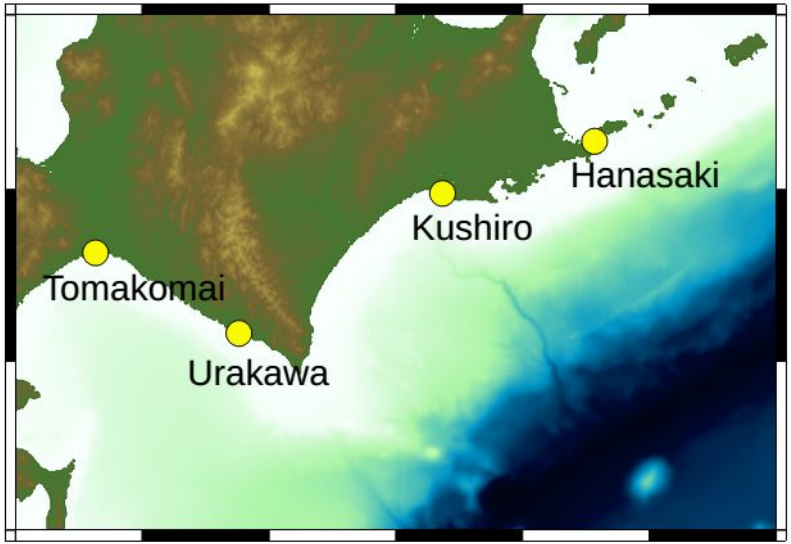

Tomakomai: **Five tsunami events have different behaviors on the spectrum.**. For the 2010 event, the peak of the spectrum is 85.7 min, but for the 1730 event, there is another evident spectral peak at 33.1 min. The energy distribution is more even among different periods with regard to 1906, 1960 and 1964 events.

3. Results: Modal Analysis of Tide Gauges at Hokkaido Region

Representative Eigenmodes

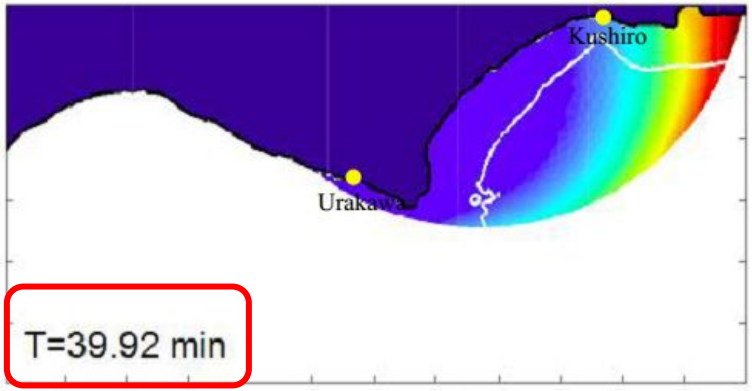

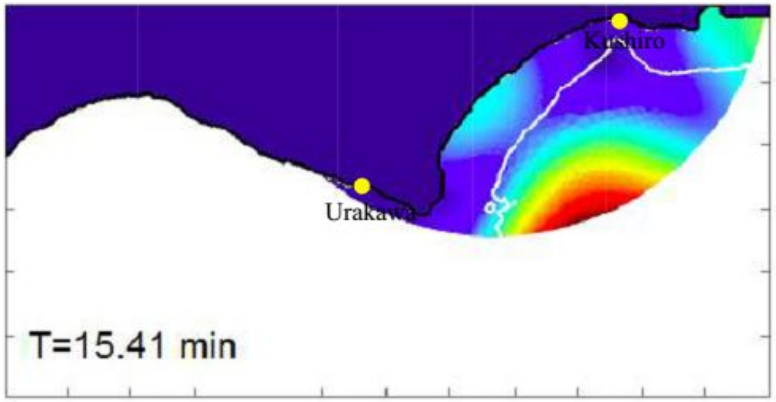

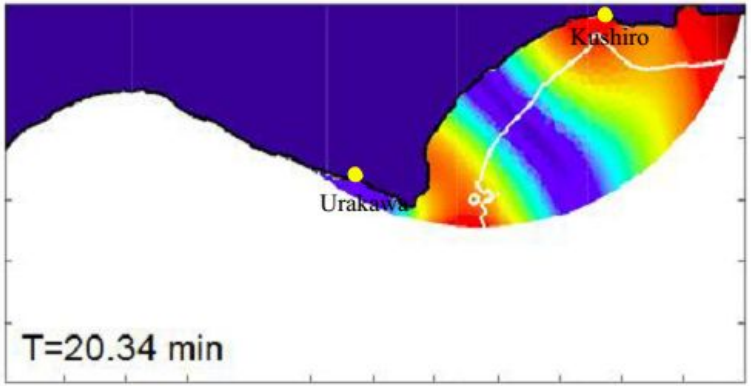

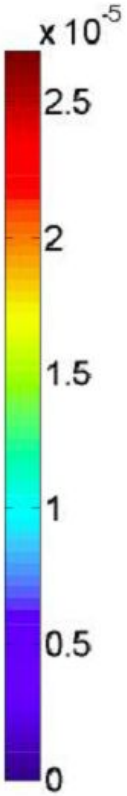

* The white line in the figures indicates the 200-m contour line.
** The modes of Hanasaki and Tomakomai are not calculated due to the limitation of the code (Cortes et al., 2017).

3. Results: Spectral Analysis of Tide Gauges at Sanriku Region

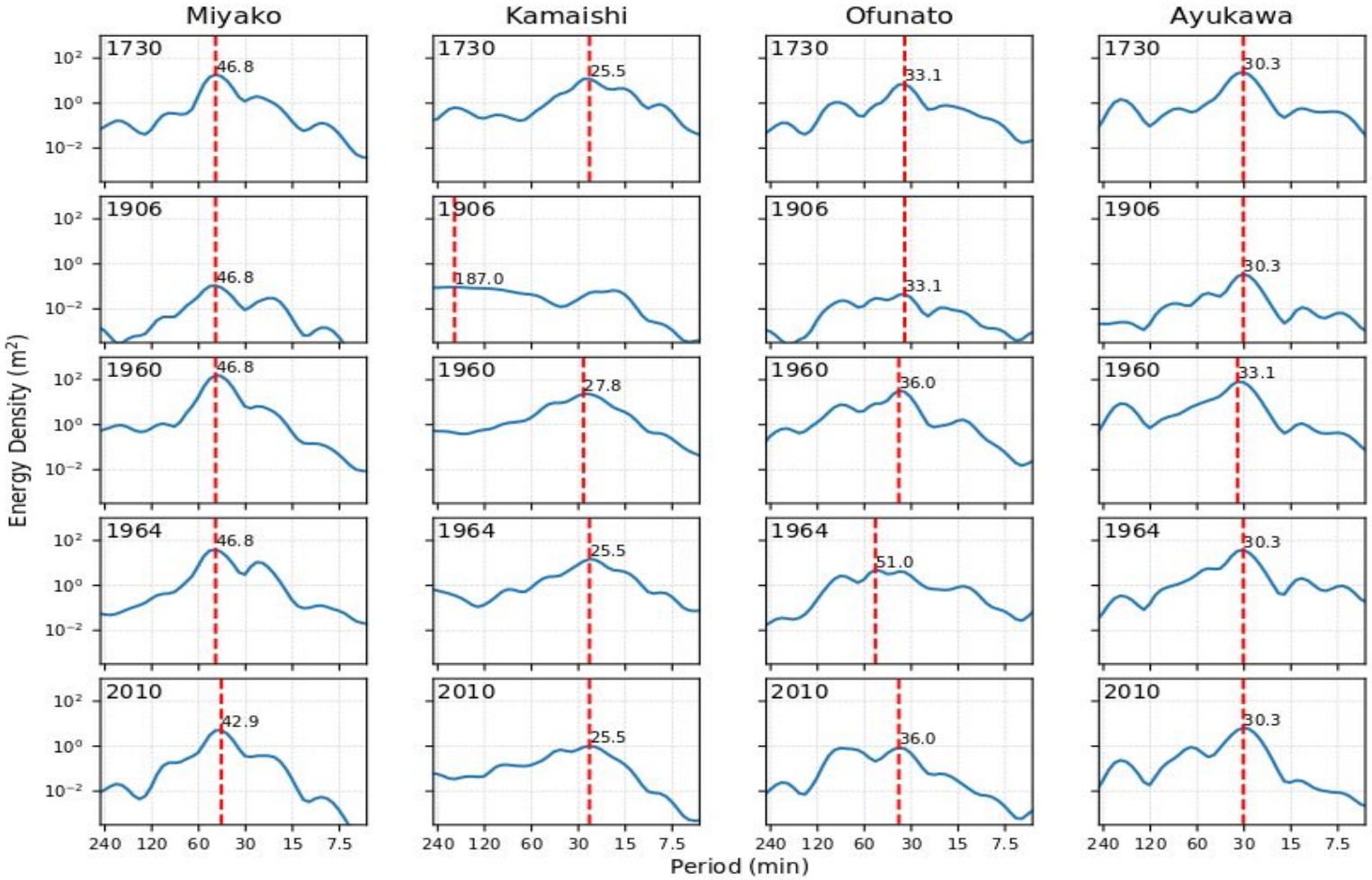

Tide Gauges at Sanriku Region

Miyako: **All tsunami events have similar frequency response** (42.9 min to 46.8 min).

Kamaishi: **The 1906 tsunami event has a different response from other events** (20 min). For the other four events, they have a slightly larger amplitude in the high-period part (> 120 min).

Ofunato: **All tsunami events have similar frequency response.** There are two small peaks on the spectrum, one at around 30 min, another at around 90 min.

Ayukawa: **All tsunami events have similar frequency response** (30 min to 33.3 min).

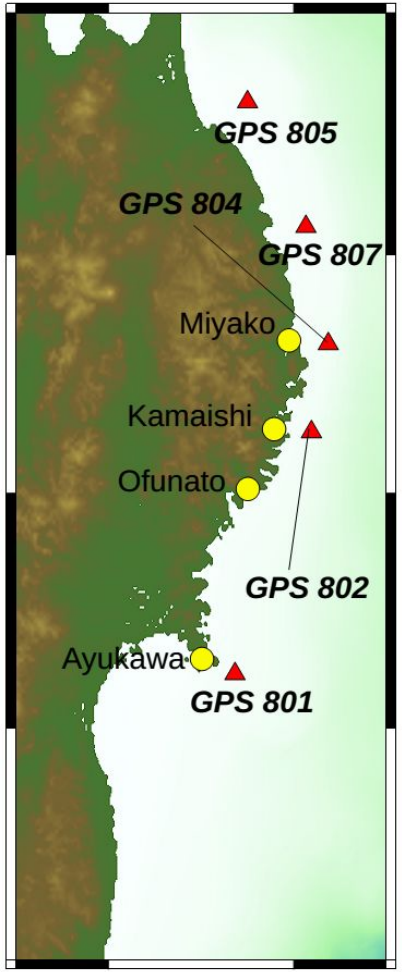

3. Results: Modal Analysis of Tide Gauges at Sanriku Region

Representative Eigenmodes

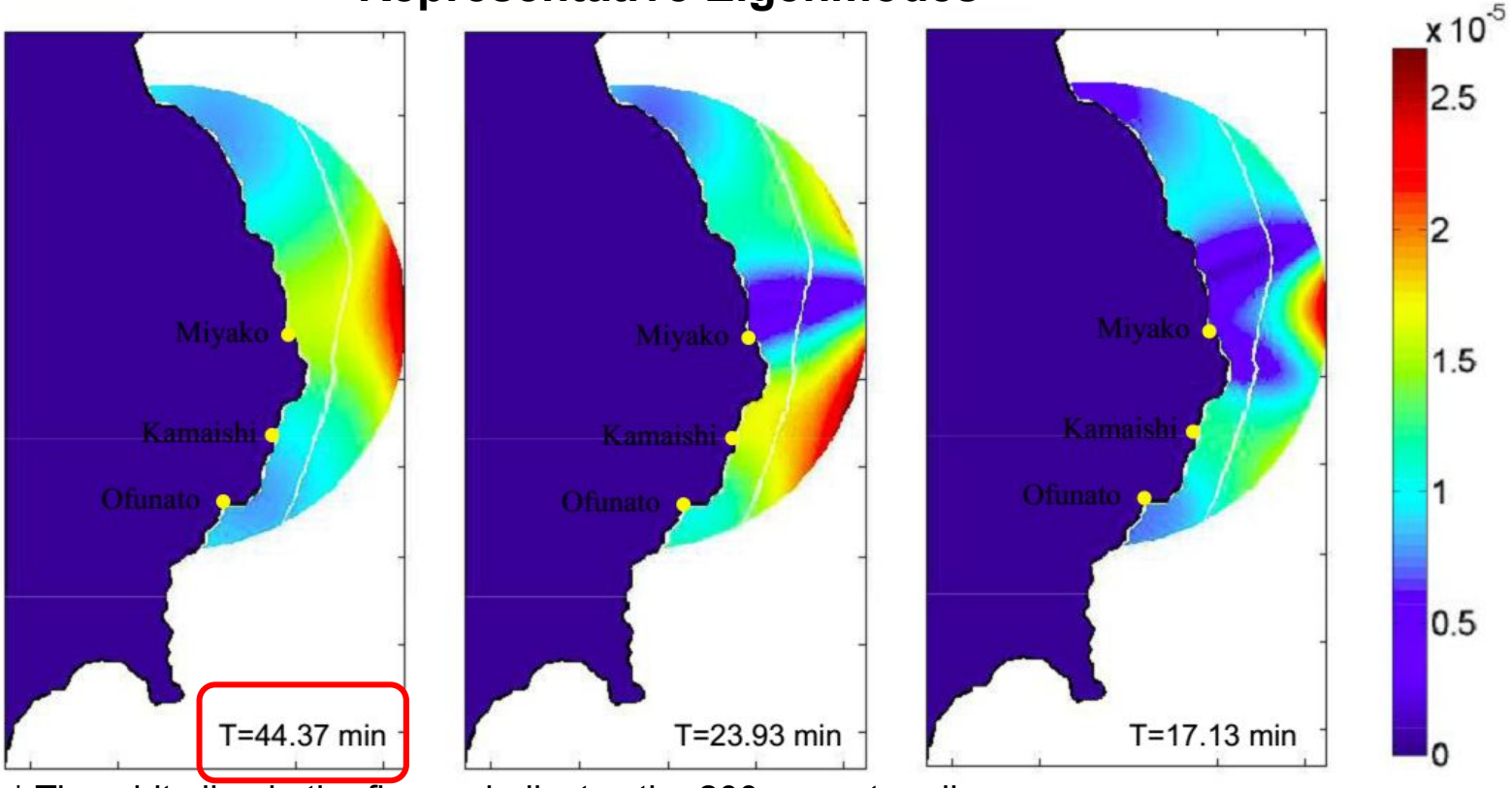

* The white line in the figures indicates the 200-m contour line.

** The modes of Ayukawa is not calculated due to the limitation of the code (Cortes et al., 2017).

3. Results: Spectral Analysis of GPS Gauges at Sanriku Region

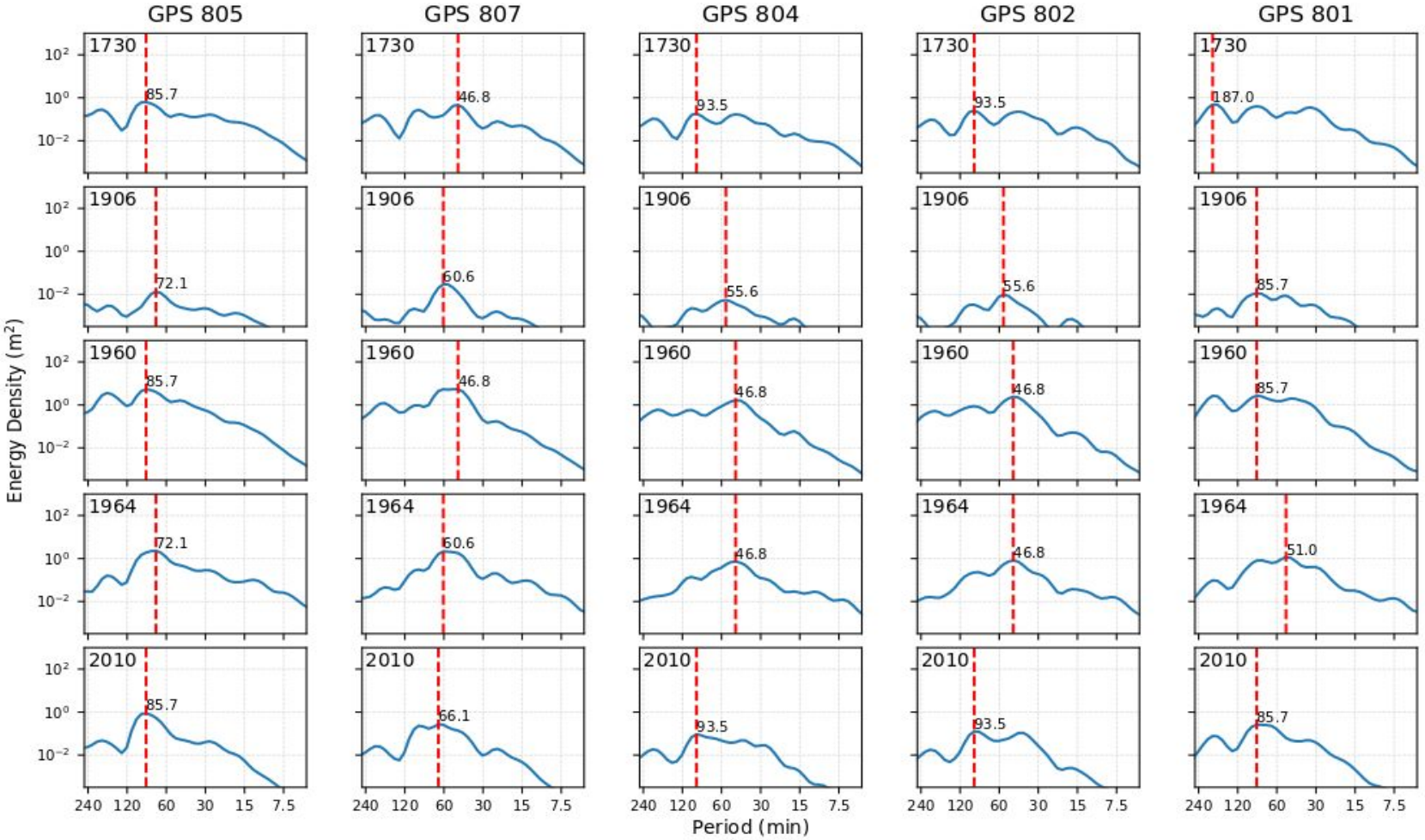

GPS 805: **All tsunami events have similar frequency response** (72.7min to 85.7 min).

GPS 807: **All tsunami events have similar frequency response** (51.0 min to 66.1 min).

GPS 804: **Five tsunami events have different behaviors on the spectrum.** The spectrum of the 1730 event has twos peak at around 40 min and 90 min. The 1906 event has only one peak at 55.6 min. The 1960 and 1964 events has one peak at 46.8 min. The 2010 event has a peak at 93.5 min.

GPS 802: **Five tsunami events have different behaviors on the spectrum.** The spectrum of the 2010 event is quite smooth, with a prominent period of 85.7 min. However, for the 1906, 1960 and 1964 events the peaks are 55.6 min, 46.8 min and 46.8 min.

GPS 801: **Five tsunami events have different behaviors on the spectrum.** For the 2010 event, the spectrum has a prominent period of 85.7 min. The 1730 and 1960 events have three peaks, at around 180 min, 90 min and 40 min.

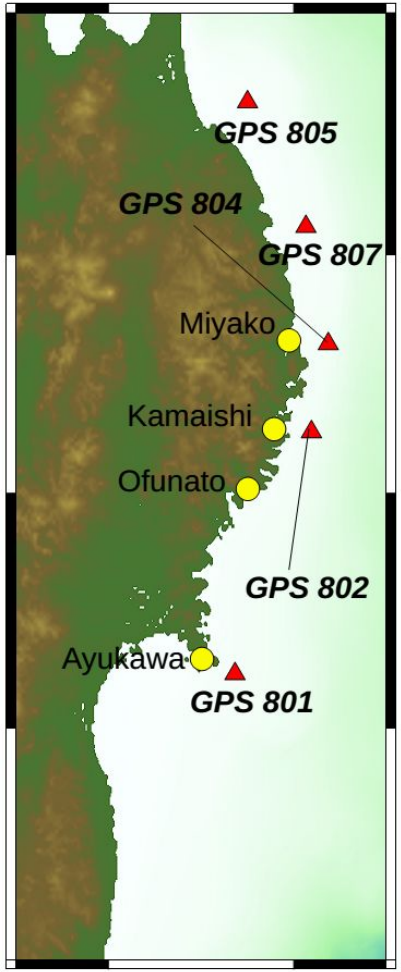

4. Conclusions & Future Work

1. Tide gauges usually have a similar spectrum shape of different tsunami events. They are more affected by local bathymetry.
2. GPS gauges off southern Sanriku region have different behaviors on the spectrum, while those off northern northern Sanriku region have similar spectrum shape.
3. The period of the eigenmode of free oscillation is consistent with the waveform spectral analysis.

Our next step:

★ To determine the tsunami wavelengths and calculate the dominant periods.
★ To include the analysis of DART records.
★ To Compare the results of different slip distribution 1730-like events for a systematic comparison of the effects.

Acknowledgement & References

YW has been funded by KAKENHI JP19J20293 and the SEELA funds. MQ, NZ and RC has been funded by the Centro de Investigación para la Gestión Integrada del Riesgo de Desastres, ANID/FONDAP/1511007. NZ has been partially funded by the CYCLO Millennium Nucleus the Seismic Cycle Along Subduction Zones, Chile.

Bellotti, G., Briganti, R., et al. (2012). The combined role of bay and shelf modes in tsunami amplification along the coast, *J. Geophys. Res.*, 117, C08027. https://doi.org/10.1029/2012JC008061.

Carvajal, M., Cisternas, M., & Catalán, P. A. (2017a). Source of the 1730 Chilean earthquake from historical records: Implications for the future tsunami hazard on the coast of Metropolitan Chile, *J. Geophys. Res. Solid Earth*, 122, 3648-3660. https://doi.org/10.1002/2017JB014063.

Rabinovich, A. B. (2010). Seiches and harbor oscillations. In *Handbook of Coastal and Ocean Engineering* (pp. 193–236). https://doi.org/10.1142/9789813204027_0011.

Torrence, C., & Compo, G. P. (1998). A practical guide to wavelet analysis. Bull. Am. Meteorol. Soc., 79, 61–78. https://doi.org/10.1175/1520-0477(1998)079<0061:APGTWA>2.0.CO;2.

Yamanaka, Y., Tanioka, Y., & Shiina, T. (2017). A long source area of the 1906 Colombia–Ecuador earthquake estimated from observed tsunami waveforms, *Earth Planets Space*, 69:163. https://doi.org/10.1186/s40623-017-0750-z.

Thank you and Take Care!